

# Introduction to Topological Quantum Computation \*

Jiannis K. Pachos

School of Physics and Astronomy,  
University of Leeds, Leeds LS2 9JT, UK

E-mail: [j.k.pachos@leeds.ac.uk](mailto:j.k.pachos@leeds.ac.uk)

---

\*Copyright (C) 2010: Permission is granted to everyone to make verbatim copies of this document provided that the copyright notice and this permission notice are preserved.



# Synopsis

- **Introduction to anyons and topological models**

Anyons, their properties and their relation to topological quantum computation.

- **Quantum double models**

Quantum double models are stabilizer codes, that can be described very much like quantum error correcting codes. They include the toric code and various Abelian and non-Abelian extensions.

- **The Jones polynomials**

Jones polynomials are topological invariants of links and knots that are related to anyons. Their evaluations by classical algorithms is computationally complex but their approximation by quantum algorithms is efficient.

- **Outlook**

Overview of the current state of topological quantum computation and open questions.

## Recommended Literature

- G. K. Brennen and J. K. Pachos, “Why should anyone care about computing with anyons?”, *Proceedings of the Royal Society A* **464**, 1-24 (2008), arXiv:0704.2241.
- M. H. Freedman, A. Kitaev, M. J. Larsen, Z. Wang, “Topological Quantum Computation”, arXiv:quant-ph/0101025 (2001).
- J. Preskill, *Lecture Notes for Physics 219: Quantum Computation*, Chapter 9, Topological Quantum Computation, <http://www.theory.caltech.edu/people/preskill/ph229/>.
- Various materials can be found at: <http://quantum.leeds.ac.uk/~jiannis/>.

## Acknowledgements

I would like to thank my students Ville Lahtinen, James Wootton and Abbas Al Shimary for careful reading of the notes as well as Gavin Brennen and Almut Beige for many inspiring direct and indirect contributions.



# Table of Contents

<b>1</b>	<b>Introduction</b>	<b>1</b>
1.1	Statistics for Quantum Computation . . . . .	1
1.2	Anyons Anyone? . . . . .	2
1.2.1	Braiding in Three and Two Dimensions . . . . .	2
1.2.2	Aharonov-Bohm Effect and Berry Phases . . . . .	3
1.3	Fusion and Braiding Properties of Anyons . . . . .	5
1.4	Anyonic Quantum Computation . . . . .	9
1.5	Example: Fibonacci Anyons . . . . .	10
1.6	Exercises . . . . .	12
<b>2</b>	<b>Quantum Double Models</b>	<b>13</b>
2.1	From Error Correction to Topological Models . . . . .	13
2.1.1	Quantum Error Correction . . . . .	13
2.1.2	Stabilizer Formalism . . . . .	14
2.1.3	Topological Models . . . . .	14
2.2	Quantum Double Models . . . . .	15
2.2.1	The Simple Case of the Toric Code . . . . .	15
2.2.2	General $D(G)$ Quantum Double Models . . . . .	18
2.3	Example: The $D(S_3)$ Model . . . . .	20
2.4	Exercises . . . . .	21
<b>3</b>	<b>Jones Polynomials</b>	<b>23</b>
3.1	A New Quantum Algorithm! . . . . .	23
3.2	Braid Group and Traces . . . . .	23
3.3	Reidemeister Moves and Skein Relations . . . . .	25
3.4	Analog Evaluation of Jones Polynomials . . . . .	26
3.5	Example: A Simple Link . . . . .	27

3.6 Exercises . . . . .	27
<b>4 Outlook</b>	<b>29</b>
4.1 Topological Entropy . . . . .	29
4.2 Topological Memories . . . . .	31
4.3 Anyons: Where Are They? . . . . .	31
4.4 Exercises . . . . .	32

# Chapter 1

## Introduction

### 1.1 Statistics for Quantum Computation

Physics should remain unchanged if we exchange two identical particles. This is a fundamental symmetry with far reaching consequences. In three dimensions it dictates the existence of bosons and fermions. Their wave function acquires a  $+1$  or a  $-1$  phase, respectively, whenever two particles are exchanged. In one dimension the exchange of particles causes them inevitably to collide. When one considers two dimensions, a variety of statistical behaviors is possible. Apart from bosonic and fermionic behaviors, arbitrary phase factors, or even non-trivial unitary evolutions, can be obtained when two particles are exchanged [1]. Particles with such an exotic statistics are called anyons.

The study of anyons started as a theoretical construction of two dimensional models [2]. It was soon realized that they can be encountered in physical systems with effective two dimensional behavior. For example, confined gases of electrons in two dimensions in the presence of sufficiently strong magnetic field and low temperatures give rise to the Fractional Quantum Hall Effect [3, 4, 5]. The low energy excitations of these systems are localized quasiparticle excitations that can actually exhibit anyonic statistics. Alternatively, one can engineer two dimensional spin lattice models with quasiparticles that exhibit anyonic statistics.

Systems that support anyons are called topological as their properties depend on global characteristics and not on local details. They have highly entangled degenerate ground states that give rise to their exotic behavior. The order parameters that detect the topological phases of systems are non-local, in contrast e.g. to magnetization. Various smoking guns exist for topological order, such as ground state degeneracy, topological entropy or the explicit detection of anyons. As topological order comes in various forms [6], the study and characterization of topological systems in their generality is complex and still an open problem.

Quantum computation requires the encoding of quantum information and its manipulation with quantum gates [7]. Qubits, the quantum version of classical bits, provide a two dimensional Hilbert space. Quantum gates are necessary to manipulate information and to perform a computation. A universal quantum computer employs a sufficiently large set of

gates in order to perform arbitrary quantum algorithms. In recent years, there have been two main quests for quantum computation: to find new algorithms, i.e. beyond searching [8] and factorizing [9], and to perform fault-tolerant evolutions.

There have been several proposals of quantum computation that are conceptually different, but equivalent to the circuit model. One way quantum computation [10] starts from a large entangled state. Information is processed by single qubit measurements, which contrasts the popular belief that quantum computation must be reversible. Adiabatic quantum computation is another way of processing information [11]. There, the answer to the problem is encoded into the unique ground state of a Hamiltonian. Then an adiabatic evolution of a simple starting Hamiltonian with a known ground state is considered. The ground state of the final Hamiltonian is a bit string encoding the answer to a problem.

In the nineties a surprising connection was made. It was argued that anyons could be employed to perform quantum computation [12]. Kitaev [13] demonstrated that anyons could actually be used to perform fault-tolerant quantum computation. This was a very welcomed advance as errors are present in any physical realization of quantum computation, coming from the environment or from control imperfections. Shor [14] and Steane [15] independently demonstrated that for sufficiently isolated quantum systems and for sufficiently precise quantum gates, quantum error correction can allow fault-tolerant computation. However, the required limits are too stringent and demand a large overhead in qubits and quantum gates. In contrast to this, anyonic quantum computation promises to resolve the problem of errors from the hardware level.

Topological systems can serve as quantum memories and as quantum computers. One can encode quantum information in simple topological systems in such a way that it is shielded from environmental perturbations. This is an important property for constructing quantum hard disks. Complex enough topological systems can realize quantum computation. They can manipulate information with very accurate quantum gates, while keeping the information protected at all times. In these systems, information is encoded in the possible outcomes when bringing two anyons together. The exchange of anyons gives rise to statistical logical gates. Fundamental properties of the quasiparticles can thus become the means to perform quantum computation. Fault-tolerance stems from the ability to keep the quasiparticles intact. The result is a surprisingly effective and aesthetically appealing method for performing fault-tolerant quantum computation.

## 1.2 Anyons Anyone?

### 1.2.1 Braiding in Three and Two Dimensions

It is commonly accepted that point-like particles, elementary or not, come in two species: bosons or fermions. These statistical behaviors can be obtained by circulating a particle around an identical one and observing the topological characteristics of their evolution. In three dimensions this evolution spans a path  $\gamma_1$  that can be continuously deformed to  $\gamma_2$ , as seen in Figure 1.1, and then to a trivial path. As a consequence the wave function,  $|\Psi(\gamma_1)\rangle$ , of the system after the circulation has to be exactly the same as the original one  $|\Psi(0)\rangle$ ,

i.e.

$$|\Psi(\gamma_1)\rangle = |\Psi(\gamma_2)\rangle = |\Psi(0)\rangle. \quad (1.1)$$

It is easily seen that a full circulation is effectively equivalent to two successive particle exchanges. Thus, a single exchange can result in a phase factor  $e^{i\varphi}$  that has to square to unity in order to be consistent with (1.1), giving, finally,  $\varphi = 0, \pi$ . These two cases correspond to the bosonic and fermionic statistics, respectively.

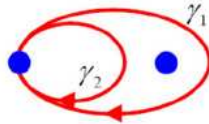


Figure 1.1: A particle spans a loop around another one. In three dimensions it is possible to continuously deform the path  $\gamma_1$  to the path  $\gamma_2$  which is equivalent to a trivial path.

When we restrict ourselves to two spatial dimensions, then there are more possibilities in statistical behaviors. If the particle circulation  $\gamma_1$  of Figure 1.1 is performed on a plane, then it is not possible to continuously deform it to the path  $\gamma_2$ . Still the evolution that corresponds to  $\gamma_2$  is equivalent to the trivial evolution as seen in Figure 1.2. As we are not able to deform the evolution of path  $\gamma_1$  to the trivial one the above argument does not apply. Actually, it is possible to assign an arbitrary phase factor, or even a whole unitary, to this evolution. Thus, particles in two dimensions can have richer statistical behaviors, possibly different from bosons or fermions.

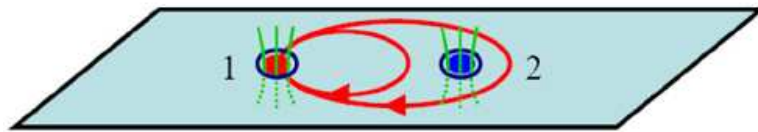


Figure 1.2: In two dimensions the two paths  $\gamma_1$  and  $\gamma_2$  are topologically distinct. This gives the possibility of having non-trivial phase factors appearing when one particle circulates the other. This can be visualized by having the particles carrying electric charge as well as magnetic flux which is known to give rise to the Aharonov-Bohm effect.

### 1.2.2 Aharonov-Bohm Effect and Berry Phases

The statistical phases of anyons can be viewed as Aharonov-Bohm phases or as Berry phases. While these descriptions might inspire some readers they are not fundamental in understanding the properties of anyons. To visualize the behavior of anyons one should think of them as being composite particles consisting of a magnetic flux  $\Phi$  and a ring of electric charge  $q$ , as depicted in Figure 1.2. If particle 1 circulates particle 2, then its charge  $q$  goes around the flux  $\Phi$ , thereby acquiring a phase factor  $U = e^{iq\Phi}$ . This is known as

the Aharonov-Bohm effect [16], which gives rise to the magnetic field  $\mathbf{B} = \nabla \times \mathbf{A}$  and the corresponding flux,  $\Phi$ , through

$$\Phi = \oint_{\gamma} \mathbf{A} \cdot d\mathbf{l} = \iint_S \nabla \times \mathbf{A} \cdot d\mathbf{s} = \iint_S \mathbf{B} \cdot d\mathbf{s}. \quad (1.2)$$

Here  $\gamma$  is the spanned looping path,  $d\mathbf{l}$  is an elementary segment of the path,  $S$  is a surface enclosed by  $\gamma$  and  $d\mathbf{s}$  is its element. Even though the vector field,  $\mathbf{A}$ , can be non-zero on the whole plane, the magnetic flux is confined at the neighborhood of the anyon 2. Hence the resulting phase factor  $U = e^{iq\Phi}$  does not depend on the details of the path of particle 1. It depends only on the number of times it circulates around it. Hence, it is topological in nature and it can faithfully describe the mutual statistics of the particles. The statistical angle of these anyons is  $\varphi = q\Phi/2$ .

Non-Abelian charges and fluxes generate unitary matrices  $U$  instead of phase factors. In this case a circulation of one anyon around another can lead to its final state being in superposition. The anyons that have such statistics are called non-Abelian, while anyons that obtain a simple phase factor are called Abelian. In reality the presence of charge and flux come from an effective, emerging gauge theory that describes the low energy behavior of the model [17].

The connection between the physical system and the effective gauge theory is best formulated in terms of the geometrical Berry phase [18, 19]. To define the Berry phase consider a Hamiltonian  $H(t)$  that changes in time through a set of time dependent parameters  $\lambda^\mu$  with  $\mu = 1, \dots, m$ . For simplicity, we initiate the system in its ground state with energy  $E_0 = 0$  and assume there is a finite energy gap  $\Delta E$  separating it from the excited states. If one changes the parameters  $\lambda$  slowly in time compared to the energy gap  $\Delta E$  then the evolution is adiabatic, causing no population transfer to the excited states. If there are many degenerate ground states,  $\{|\psi^\alpha\rangle, \alpha = 1, \dots, n\}$  then the spanning of a loop  $\gamma$  in the parameters  $\lambda$  results in a non-Abelian Berry phase given by

$$\Gamma_A(\gamma) = \mathbf{P} \exp \oint_{\gamma} \mathbf{A} \cdot d\lambda, \quad (1.3)$$

where  $\mathbf{P}$  denotes path ordering. The resulting evolution is an element of  $U(n)$  evolving the ground state of the system in the following way  $\Psi(\gamma) = \Gamma_A(\gamma)\Psi(0)$ . The connection is a matrix with components given by

$$(A_\mu)^{\alpha\beta} = \langle \psi^\alpha(\lambda) | \frac{\partial}{\partial \lambda^\mu} | \psi^\beta(\lambda) \rangle. \quad (1.4)$$

This is the non-Abelian generalization of the usual Berry phase which was first presented by Wilczek and Zee [20] and reduces to the usual Berry phase for non-degenerate ground states.

Topological systems are many-body systems with localized quasiparticle excitations. The control parameters  $\lambda^\mu$  of topological systems are identified with the coordinates of the quasiparticle. When these quasiparticles are braided, their evolution can be described by a geometrical phase that is independent of the shape of the path, thus simulating the

Aharonov-Bohm effect. This topological characteristic makes the corresponding evolutions to be representations of the braid group. It has been explicitly demonstrated by Arovas, Schrieffer and Wilczek [21], how the statistics of Abelian anyons, appearing in the Fractional Quantum Hall Effect, can be expressed as such a Berry phase. The non-Abelian statistics from Berry phases was considered by Read [22] and Lahtinen and Pachos [23].

### 1.3 Fusion and Braiding Properties of Anyons

As the statistical properties dominate the behavior of the anyonic states, it is convenient to employ the world lines of the particles to keep track of their positions (see Figure 1.3). We assume that we can trap and move the anyons around the plane leading to world lines in  $2 + 1$  dimensions. Exchanges of the anyons can be easily described by just braiding their world lines. We can also depict the pair creation of anyons from the vacuum as well as their fusion when they are brought together. The fusion gives new anyons that correspond to the possible outcomes when the original anyons are combined together.

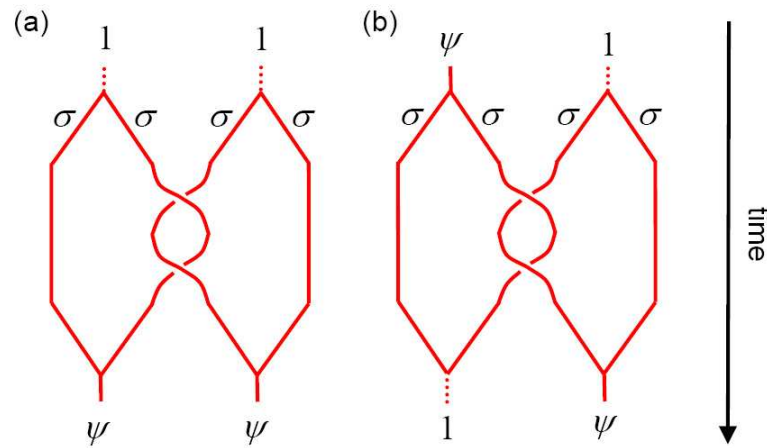


Figure 1.3: The world lines of the Ising anyons where the third dimension depicts time running downwards. (a) From the vacuum two pairs of Ising anyons are generated depicted by  $(\sigma, \sigma)$  and  $(\sigma, \sigma)$ . Then an anyon from each pair are braided by circulating one around the other. Finally, the anyons are pairwise fused, but they do not necessarily return to the vacuum. In the case of Ising  $\sigma$  anyons the fusion outcomes are fermions  $\psi$ . (b) A similar evolution, where two pairs of  $\sigma$  Ising anyons are created from a fermion  $\psi$  and the vacuum 1. The braiding causes the teleportation of the fermion between the two pairs.

To illustrate these properties let us consider the Ising anyonic model with particle types 1 (vacuum),  $\sigma$  (non-Abelian anyon) and  $\psi$  (fermion). These can be thought of as conserved quantum numbers of the quasiparticles. The conservation of these quantum numbers is given by the following fusion rules

$$\sigma \times \sigma = 1 + \psi, \quad \sigma \times \psi = \sigma, \quad \psi \times \psi = 1,$$

with 1 fusing trivially with the rest of the particles ( $\sigma \times 1 = \sigma$  and  $\psi \times 1 = \psi$ ). The first fusion rule signifies that if we bring two  $\sigma$  anyons together they might annihilate (i.e.  $\sigma$  is its own antiparticle) or they can give rise to the fermion  $\psi$  depending on their total state. Hence, the fusion of two  $\sigma$ 's has two possible channels. The second fusion rule indicates that fusing a  $\psi$  with a  $\sigma$  gives back a  $\sigma$ . The third states that when two fermions are brought together they are fused to the vacuum.

Assume that one creates from the vacuum two pairs of anyons  $(\sigma, \sigma)$  as seen in Figure 1.3(a). Then the fusion rules imply that the generation of anyons results in a well defined pair of anyon anti-anyon. The state of these anyons can be denoted as  $|\sigma, \sigma \rightarrow 1\rangle$  indicating that if we fuse back these anyons their fusion outcome is known. In general, when two arbitrary anyons are fused, it is possible to have various outcomes depending on their total state. In Figure 1.3(a), one can see that the fusions result in  $\psi$  anyons. For this fusion outcome we define the state  $|\sigma, \sigma \rightarrow \psi\rangle$ . It corresponds to the case where two anyons of type  $\sigma$  fuse to the fermion  $\psi$  when brought together. The states  $|\sigma, \sigma \rightarrow 1\rangle$  and  $|\sigma, \sigma \rightarrow \psi\rangle$  give rise to a two dimensional Hilbert space, the fusion space. As seen in Figure 1.3(a) it is possible to evolve the initially prepared state of  $\sigma$  anyons from the state  $|\sigma, \sigma \rightarrow 1\rangle \otimes |\sigma, \sigma \rightarrow 1\rangle$  to the state  $|\sigma, \sigma \rightarrow \psi\rangle \otimes |\sigma, \sigma \rightarrow \psi\rangle$ . Due to the conservation of the total type of particles we need to keep track of the particles of one pair only. Hence, the braiding evolution can be described by a two dimensional matrix that rotates the fusion states from  $|\sigma, \sigma \rightarrow 1\rangle$  to  $|\sigma, \sigma \rightarrow \psi\rangle$  up to an overall phase.

In general, the fusion rules are given by

$$a \times b = N_{ab}^c c + N_{ab}^d d + \dots, \quad (1.5)$$

where anyons  $a$  and  $b$  are fused to produce anyon  $c$  or  $d$  or any other possible outcome. The integers  $N_{jk}^l$  denote the multiplicity with which the particles  $l$  are generated when fusing particles  $j$  and  $k$ . This procedure is similar to the tensor product notation of spins that results in a new spin basis, e.g.  $\frac{1}{2} \otimes \frac{1}{2} = 0 \oplus 1$ . Abelian anyons, in particular, have only a single fusion channel  $a \times b = c$  so their fusion space is one dimensional. Non-Abelian anyons have necessarily multiple fusion channels that gives rise to higher dimensional fusion spaces.

The Hilbert space,  $\mathcal{M}_{(n)}$ , corresponding to  $n$  anyons  $(a_1, \dots, a_n)$  has dimension

$$\dim(\mathcal{M}_{(n)}) = \sum_{b_1 \dots b_{n-2}} N_{a_1 a_2}^{b_1} \dots N_{b_{n-2} a_n}^{b_{n-1}}. \quad (1.6)$$

The representation of the fusion states is given by  $|a, b \rightarrow c; \mu\rangle$ , where  $\mu = 1, \dots, N_{ab}^c$  parameterizes possible multiplicity in a certain fusion channel. In the case of Ising anyons the only non-zero fusion coefficients are  $N_{\sigma\sigma}^1 = 1$ ,  $N_{\sigma\sigma}^\psi = 1$ ,  $N_{1\sigma}^\sigma = 1$  and  $N_{\psi\sigma}^\sigma = 1$ . For example, substituting  $a_1 = a_2 = a_3 = c = \sigma$  in equation (1.6) and having the summation running over  $b_1 = 1, \psi$  it gives  $\dim(\mathcal{M}_{(4)}) = 2$  as expected.

There is an alternative way to compute the dimension of  $\mathcal{M}_{(n)}$  corresponding to  $n$  identical anyons,  $a$ , using the concept of *quantum dimension*. The quantum dimension  $d_a$  quantifies the rate of growth of Hilbert space dimension  $\dim(\mathcal{M}_{(n)}) \rightarrow d_a^n$  when one additional  $a$  particle is inserted for large  $n$ . Starting from the fusion rules one can show

that the quantum dimension satisfies the following relation

$$d_a d_b = \sum_c N_{ab}^c d_c.$$

For the case of the Ising model the quantum dimension of the  $\psi$ 's is given by  $d_\psi^2 = 1 \Rightarrow d_\psi = 1$ . For the  $\sigma$ 's we have  $d_\sigma^2 = 1 + d_\psi \Rightarrow d_\sigma = \sqrt{2}$ .

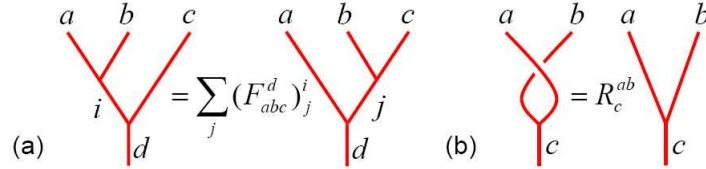


Figure 1.4: Fusion and braiding properties. (a) When the order of fusion between three anyons,  $a$ ,  $b$  and  $c$  with outcome  $d$  is changed then a rotation in the fusion space is performed given by the matrix  $F_{abc}^d$ . This corresponds to a change of basis in the fusion space. (b) A braiding operation between anyons  $a$  and  $b$  with fusion outcome  $c$  gives the phase  $R_c^{ab}$ .

It is possible to access the fusion space by certain operations on the anyons. These are physically allowed operations given by changes in the fusion order, that correspond to basis change, and exchanges, or braids, leading to non-trivial evolutions. For example, one can fuse the anyons  $a$ ,  $b$  and  $c$  in two distinctive ways. One can first fuse  $a$  with  $b$  and then their outcome with  $c$  or first fuse  $b$  with  $c$  and then their outcome with  $a$ . As shown in Figure 1.4(a), these two processes are related by a unitary matrix with elements  $(F_{abc}^d)^i_j$ . The  $F$  matrix facilitates between the change of basis in the fusion space. For the case of the Ising model, the  $F$  matrix is given by

$$F_{\sigma\sigma\sigma}^\sigma = \frac{1}{\sqrt{2}} \begin{pmatrix} 1 & 1 \\ 1 & -1 \end{pmatrix} \quad (1.7)$$

in the  $\{1, \psi\}$  basis.

To manipulate the states of the fusion space, one can braid the anyons before fusing them. This operation is described by the diagonal  $R$  matrix, depicted in Figure 1.4(b). In the case of two  $\sigma$  Ising anyons the components of the  $R$  matrix are given by  $R_1^{\sigma\sigma} = e^{-i\pi/8}$  and  $R_\psi^{\sigma\sigma} = e^{-i3\pi/8}$  [24]. That is, the fermionic fusion channel acquires an additional phase  $\pi/2$  during the  $\pi$  rotation due to the spin  $1/2$  nature of the fermion. The superposition of multiple fusion outcomes in the braiding process results in unitary operations.

Return now to Figure 1.3(a). Initially, we pair create two anyonic pairs. Then two anyons, one from each pair, are braided by circulating one around the other. Finally, the corresponding pairs are fused. The fusion may not result in the vacuum as the braiding process could change the internal state of the anyons. Indeed, for the case of the Ising anyons the outcome of the fusion is  $\psi$  in both cases. These  $\psi$ 's can be further fused giving the vacuum that we had started with in agreement with the conservation of the total quantum

numbers. Nevertheless, the braiding has dramatically changed the internal fusion space of each pair, even though they have not been in contact. Figure 1.3(b) shows the generation of one pair of Ising anyons from a fermion and another one from the vacuum. The braiding process causes the fermion to be teleported from one pair to the other. Such non-trivial unitary rotations of the fusion space are possible in the case of non-Abelian anyons by braiding operations.

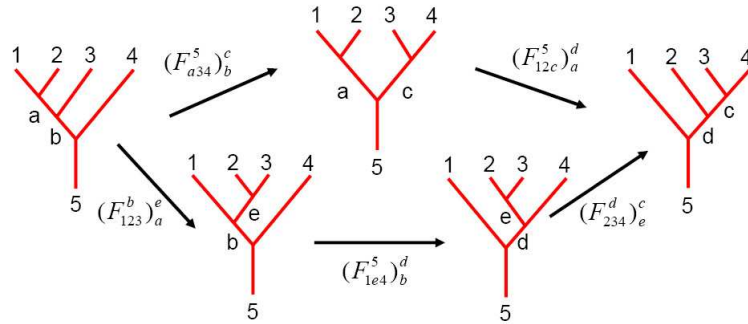


Figure 1.5: The pentagon identity. Starting from a four anyon combination, a sequence of five fusion rearrangements returns to the original configuration. It is taken as an axiom that this sequence is the identity mapping.

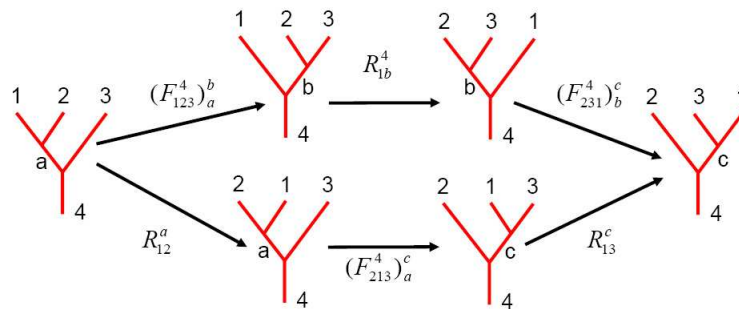


Figure 1.6: The hexagon identity. It is relating the fusion of three anyons by a sequence of fusion rearrangements and braiding operations.

Finally, one can show that consistency equations can be considered that give a relation between statistical processes and fusion relations. These consistency equations are called pentagon and hexagon equations [25] due to their geometrical interpretation (see Figure 1.5 and Figure 1.6, respectively). They are the subject of study of Topological Quantum Field Theory [26]. From the pentagon rule, the following relation between the elements of the  $F$

matrices is obtained,

$$(F_{12c}^5)_a^d (F_{a34}^5)_b^c = \sum_e (F_{234}^d)_e^c (F_{1e4}^5)_b^d (F_{123}^b)_a^e. \quad (1.8)$$

Similarly, from the hexagon rule

$$\sum_b (F_{231}^4)_b^c R_4^{1b} (F_{123}^4)_a^b = R_c^{13} (F_{213}^4)_a^c R_a^{12}. \quad (1.9)$$

Consistent anyon models are characterized by some  $R$ - and  $F$ -matrices. which have to satisfy these polynomial equations. Conversely, the solutions of these two polynomial equations give a discrete set of  $F$  and  $R$  matrices. This property, known as the Ocneanu rigidity, makes the  $R$  and  $F$  unitaries immune against small perturbations [24].

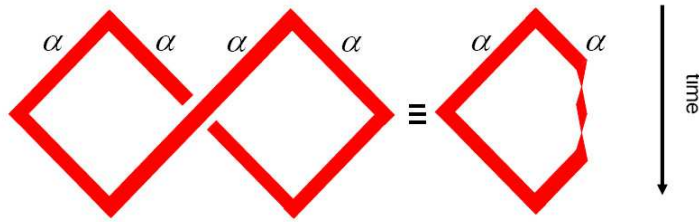


Figure 1.7: The equivalence between spin and statistics. The anyons are depicted here as ribbons to keep track of their spin rotation. Two anyons, each one from two anyon anti-anyon pairs, are exchanged and then fused to the vacuum. This process can be continuously deformed to rotating one anyon from a pair by  $2\pi$  and recombining them causing an evolution due to the spin of the anyon.

The interpretation of the anyons with world lines, and in particular with “world ribbons” makes apparent the connection between statistics and spin [27]. In Figure 1.7 we see the schematical equivalence between the process of exchanging two Abelian anyons and the rotation of an anyon by  $2\pi$ . The first is evolved by the statistical unitary  $R$  (a phase factor for Abelian anyons) and the second is expected to obtain a phase factor  $e^{i2\pi J}$ , where  $J$  is the spin of the anyon. A direct application leads to the connection between the integer spins for bosons and half integer spins for fermions. This is in agreement with the interpretation of anyons as a composite object of charge and flux. In this case the rotation of an anyon by  $2\pi$  will rotate the charge around the flux, thereby leading to the Aharonov-Bohm effect.

## 1.4 Anyonic Quantum Computation

To implement universal quantum computation consider  $n$  non-Abelian anyons of the same type  $a$ . Apart from degrees of freedom that can be measured locally, the system possesses non-local anyonic fusion degrees. The corresponding fusion Hilbert space  $\mathcal{M}_{(n)}$  encodes the

outcomes when the anyons are pairwise fused. The dimension of  $\mathcal{M}_{(n)}$  grows exponentially with the number  $n$  of anyons, i.e.  $\dim(\mathcal{M}_{(n)}) = d_a^n$ , though, this does not necessarily admit a tensor product structure. Nevertheless, a qubit tensor product subspace can always be identified, where quantum information can be encoded in the usual way.

Logical gates can be performed by braiding the anyons that gives rise to applications of the  $R$ -matrix. This operation does not affect the type of anyons neither their local degrees of freedom, but it can have a non-trivial effect on the fusion space. In combination with the  $F$ -matrices one can evolve the encoded information in a non-trivial way. When these two matrices efficiently span a dense set of unitaries acting on the qubits, the corresponding non-Abelian model can support universal quantum computation. If two anyons are brought next to each other, then part of the information of the anyonic fusion space is accessible, as their fusion channel can be determined. This procedure can be employed to finally measure the computational outcome.

The information encoded in the fusion space is not at all accessible by local operations. Hence, the environment, assumed to act in a local way, cannot alter it. This is the fault-tolerant characteristic that makes anyons a favorable medium for performing quantum computation. The environmental errors that can be avoided efficiently by the topological systems are local perturbations to the Hamiltonian. Nevertheless, probabilistic errors on the system due to a finite temperature do affect the encoded space. It is still an open problem of great interest to devise a method that can efficiently overcome temperature errors.

## 1.5 Example: Fibonacci Anyons

In this section we present the probably most celebrated non-Abelian anyonic model. This is not only due to its simplicity and richness in structure, but also to its connection to the Fibonacci series. In this model there are two different types of anyons,  $1$  (vacuum) and  $\tau$  (non-Abelian anyon), that have the following fusion rules

$$1 \times 1 = 1, \quad 1 \times \tau = \tau, \quad \tau \times \tau = 1 + \tau. \quad (1.10)$$

It is interesting to study all the possible outcomes when we fuse  $n + 1$  anyons of type  $\tau$  arranged as in Figure 1.8(a). For this we initially fuse the first two anyons, then their outcome is fused with the third  $\tau$  anyon and the single outcome is fused with the next one and so on. At each step  $i$  we assign an index  $a_i$  that indicates the outcome of the fusion at that step. The states  $|a_1, a_2, \dots, a_{n-2}\rangle$  belong to the fusion Hilbert space of the anyons,  $\mathcal{M}_{(n)}$ . These states are not all independent. As the  $\tau$  anyons have two possible fusion outcome states, it is natural to ask, in how many distinct ways,  $d_\tau(n)$ , can one fuse  $n + 1$  anyons of type  $\tau$  to yield finally a  $\tau$ . At the first fusing step the possible outcomes are  $1$  or  $\tau$ , giving  $d_\tau(2) = 1$ . When we fuse the outcome with the next anyon then  $1 \times \tau = \tau$  and  $\tau \times \tau = 1 + \tau$ , resulting to two possible  $\tau$ 's coming from two different processes and a  $1$ , i.e.  $d_\tau(3) = 2$ . Taking the possible outcome and fusing it with the next anyon gives a space of  $\tau$ 's which is three dimensional,  $d_\tau(4) = 3$ . One soon notices that the dimension of the fusion space  $\dim(\mathcal{M}_{(n)})$  when  $n$  anyons of type  $\tau$  are fused, is actually the Fibonacci series.

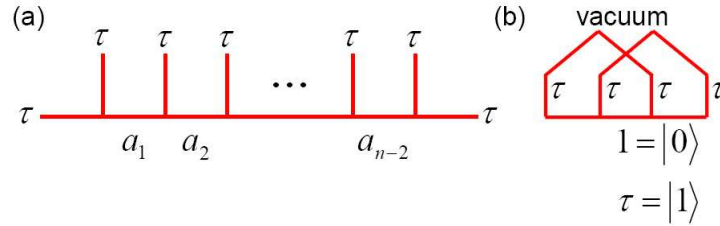


Figure 1.8: Depiction of the fusion process for anyons. (a) A series of  $\tau$  anyons are fused together ordered from left to right. The first two  $\tau$  anyons are fused and then their outcome is fused with the next  $\tau$  anyon and so on. (b) Four Fibonacci anyons in state  $\tau$  created from the vacuum can be used to encode a single logical qubit.

This dimension is given approximately by the following formula

$$\dim(\mathcal{M}_{(n)}) \propto \phi^n$$

where  $\phi \equiv (1 + \sqrt{5})/2$  is the golden mean. The quantum dimensions for the two particle types can easily be obtained from the fusion rules in Eq. (1.10):  $d_1^2 = d_1$  and  $d_\tau^2 = d_1 + d_\tau$  giving  $d_1 = 1$  and  $d_\tau = \phi$ . The golden mean has been used extensively by artists, such as Leonardo Da Vinci, in geometrical representations of nature (plants, animals or humans). It describes the ratios that are aesthetically appealing.

The Fibonacci anyonic model is a good example for realizing quantum computation. We are interested in encoding information in the fusion space of anyons and then processing it appropriately. The encoding of a qubit can be visualized by employing four  $\tau$  anyons as in Figure 1.8(b). There are two distinguishable ways the particles can be fused together that can encode the qubit,  $|0\rangle = |\tau, \tau \rightarrow 1\rangle$  and  $|1\rangle = |\tau, \tau \rightarrow \tau\rangle$ . To determine the quantum gates one needs to evaluate the  $F$  and  $R$  matrices. From the fusion rules of Fibonacci anyons and the pentagon identity one finds the non-zero values

$$\begin{aligned} (F_{\tau\tau 1}^\tau)_1^1 &= (F_{1\tau\tau}^\tau)_1^1 = (F_{\tau\tau\tau}^1)_1^1 = (F_{\tau 1\tau}^\tau)_1^1 = 1, \\ (F_{111}^1)_0^0 &= 1, F_{\tau\tau\tau}^\tau = \begin{pmatrix} \frac{1}{\phi} & \frac{1}{\sqrt{\phi}} \\ \frac{1}{\sqrt{\phi}} & -\frac{1}{\phi} \end{pmatrix}. \end{aligned}$$

These solutions are unique up to a choice of gauge. Inserting these values into the hexagon identity, one obtains the following  $R$  matrix describing the exchange of two particles

$$R = \begin{pmatrix} e^{4\pi i/5} & 0 \\ 0 & -e^{2\pi i/5} \end{pmatrix}. \quad (1.11)$$

It can be shown that the unitaries  $b_1 = R$  and  $b_2 = F_{\tau\tau\tau}^\tau R (F_{\tau\tau\tau}^\tau)^{-1}$  acting in the logical space  $|0\rangle$  and  $|1\rangle$  are dense in  $SU(2)$  in the sense that they can reproduce any element of  $SU(2)$  with accuracy  $\epsilon$  in a number of operations that scales like  $O(\text{poly}(\log(1/\epsilon)))$  [28]. Thus

an arbitrary one qubit gate can be performed as follows. Begin from the vacuum and create four anyons labelled by  $a_1, a_2, a_3, a_4$ . Braiding the first and second anyons implements  $b_1$  and braiding the second and third anyons implements  $b_2$ . A measurement of the outcome upon fusing  $a_1$  and  $a_2$  projects onto logical  $|0\rangle$  or  $|1\rangle$ . Similarly, by performing braiding over 8 anyons in state  $\tau$ , one obtains a dense subset of  $SU(d(7))$ . Since  $SU(4) \subset SU(13)$ , we can also implement any two logical qubit gate, e.g. the CNOT gate, with arbitrary accuracy. Hence the Fibonacci anyon model allows for universal computation on  $n$  logical qubits using  $4n$  physical anyons [29].

## 1.6 Exercises

- **Exercise 1:** Show that the Ising model  $F$  and  $R$  matrices satisfy the pentagon and hexagon identities. Conversely, solve the pentagon and hexagon equations given the Ising type of anyons and their fusion rules.
- **Exercise 2:** Construct the qubit space with Ising anyons and demonstrate that the  $F$  and  $R$  matrices do not provide a universal set of gates. What gates are missing? (see [30]).
- **Exercise 3:** Solve the pentagon and hexagon equations for the the  $F$  and  $R$  matrices of the Fibonacci model.
- **Exercise 4:** From the spin statistics theorem demonstrate what is the spin of the Ising and Fibonacci anyons.
- **Exercise 5:** Bratteli diagrams give a pictorial representation of the fusion outcomes of  $n$  anyons of the same type. Their horizontal axis gives the increasing number of anyons involved in the fusion and the vertical axis gives the fusion outcome. There are many distinct paths that start from the first anyon and evolve according to the choice of the fusion channels at each step. Draw all the distinct Bratteli diagrams for the Ising and Fibonacci models involving six anyons.
- **Exercise 6:** Starting from the initial vacuum state with Ising anyons can you generate entangled states?
- **Exercise 6:** Generalize the spin statistics theorem for the non-Abelian anyonic case.

## Chapter 2

# Quantum Double Models

### 2.1 From Error Correction to Topological Models

#### 2.1.1 Quantum Error Correction

Quantum error correction is the means we have to combat environmental and control errors when performing quantum computation. As errors infest any physical realization of a quantum computer the importance of quantum error correction cannot be overstated. Much in parallel to classical error correction quantum error correction works on the principle of employing a large Hilbert space to encode information in a redundant way. The goal is to perform complex encoding and decoding of information so that for low enough error rates the effect of the environment is eventually neutralized. In the following we shall review some basic properties of quantum error correction. It is pedagogical and conceptually appealing to approach topological models from the quantum error correction point of view.

Consider a Hilbert space  $\mathcal{H}$  of a quantum system spanned by  $n$  finite dimensional complex subsystems  $\mathcal{V}$ , i.e.  $\mathcal{H} = \mathcal{V} \otimes \dots \otimes \mathcal{V}$ . For simplicity, and unless it is otherwise stated, we shall initially consider a set of qubits, i.e.  $\dim(\mathcal{V}) = 2$ . The code space  $\mathcal{C}$  is a linear subspace of  $\mathcal{H}$  where the logical information is encoded. A general  $k$ -local operator  $\mathcal{O}$  is an operator that acts non-trivially to at most  $k$  subsystems of  $\mathcal{H}$  (also known as operator of length  $k$ ). Then  $\mathcal{C}$  is called a  $k$ -code if

$$\Pi_{\mathcal{C}} \mathcal{O} \Pi_{\mathcal{C}} \propto \Pi_{\mathcal{C}}, \quad (2.1)$$

where  $\Pi_{\mathcal{C}}$  is the projector on  $\mathcal{C}$ . Hence, the operator  $\Pi_{\mathcal{C}} \mathcal{O}$  is a mapping  $\mathcal{C} \mapsto \mathcal{C}$  up to a multiplicative scalar for any  $k$ -local operator  $\mathcal{O}$ . It has been shown [31] that such a code can effectively protect against errors that act on less than  $k/2$  qubits. The code is also called  $[[n, d, k]]$  where  $n$  is the total number of qubits and  $2^d$  is the dimension of the  $k$ -code  $\mathcal{C}$ . This code requires  $n$  physical qubits to encode  $d$  logical ones protected against errors that are at most  $\lfloor k/2 \rfloor$ -local. Quantum error correcting codes are commonly expressed in the stabilizer formalism which we introduce in the following.

### 2.1.2 Stabilizer Formalism

A stabilizer  $\mathbf{T}_n$  is a set of Hermitian operators,  $T_i$  with  $i = 1, \dots, n$  that commute with each other,  $[T_i, T_j] = 0$  for all  $i, j$ . The stabilized space consists of all eigenstates  $|\Psi\rangle$  with eigenvalue  $+1$  for all operators  $T_i$ . A particular example of stabilizers can be constructed from the Pauli group,  $\mathbf{P}_n$ , generated by the Pauli matrices  $\sigma^x, \sigma^y, \sigma^z$  and the identity  $\mathbb{1}$  acting on  $n$  qubits. As different Pauli operators acting on the same qubit anticommute, only a subset of the Pauli group operators commute with each other and hence form a stabilizer set. These operators are Hermitian and they square to the identity, so they have eigenvalues  $\pm 1$ . Such a maximal stabilizer set could admit a common set of  $2^n$  eigenstates uniquely identified by the pattern of the stabilizer eigenvalues. Generalizations of stabilizers to qudits are also possible. These will play a special role in the definition of the quantum double topological models presented in the following section.

One can define an error correcting code with the stabilizer formalism e.g. based on the Pauli group  $\mathbf{P}_n$ . Consider a certain commuting subgroup  $S$  of the group  $\mathbf{P}_n$ . Then the set of eigenstates of all elements of  $S$  with eigenvalue  $+1$  is the stabilizer code  $\mathcal{C}$ , where information can be stored. If  $S$  has  $s$  elements, it can encode  $d = n - s$  qubits. Any operation acting on  $\mathcal{C}$  that does not commute with  $S$  can be detected by measurements of the  $S$  observables and can be corrected. The set of operators that commute with all the elements of  $S$  is called the centralizer  $Z(S)$ . The centralizer naturally includes  $S$ , but in general has extra elements. The distance  $k$  of the code  $\mathcal{C}$  is the minimal length among the elements of  $Z(S) \setminus S$  up to a sign. Such elements serve as encoded logical operations. For an efficient encoding we thus assume that the errors are less than  $\lfloor k/2 \rfloor$ -local.

### 2.1.3 Topological Models

One can obtain topological models that support anyons by employing the error correction formalism. This facilitates the presentation of the fault-tolerant encoding of information in a physical system. Consider a general two dimensional lattice defined on a surface  $M$  and a Hamiltonian  $H = -\sum_i h_i$  with local interaction terms  $h_i$  acting on the links of the lattice. Assume that the  $h_i$  are the elements of the subgroup  $S$ . Then the ground state space of  $H$  is the stabilizer code  $\mathcal{C}$  which is  $2^d$ -dimensional and it is separated from the rest of the states by a finite energy gap. Turning an error correcting code into a Hamiltonian is a dramatic conceptual step which was first taken by Kitaev [13]. Apart from the fault-tolerant characteristics it provides a geometrical interpretation of quantum error correction, thus bringing it closer to its physical realization. Its drawback is an overhead in the number of employed qubits.

We should bear in mind that, as the error correcting procedure has been substituted by a gapped Hamiltonian that aims to penalize the generation of errors, the errors we consider here are coherent, i.e. they are perturbations to the Hamiltonian. The latter can cause virtual excitations which are automatically suppressed by keeping the characteristic size of the system large compared to the length of the perturbation. The size of the system corresponds to having a large distance  $k$  for the  $\mathcal{C}$  code, as it will become apparent in the following section. If the errors are generated by thermal noise, then the mechanism described

above cannot automatically correct them. Alternative methods have to be considered that are the subject of ongoing research.

We can demonstrate now with general arguments that particular Hamiltonians described by the error correcting formalism can actually support quasiparticles with anyonic statistics [34]. These quasiparticles are localized excitations of a Hamiltonian  $H$ . Their location  $i$  is determined from the violation of the stabilizer condition  $h_i |\Psi\rangle = |\Psi\rangle$  which corresponds to the ground state. We shall focus on the space  $\mathcal{C}$  of states that corresponds to the presence of a number of excitations. Assume that one can change the position of the quasiparticles in time by making the Hamiltonian time dependent,  $H_t$ . In particular, we are interested in the evolution of the state space  $\mathcal{C}$  when one quasiparticle is braided around another. For simplicity we discretize the time evolution of the punctures in small steps. Consider such a small step with corresponding Hamiltonians  $H_{t_i}$  and  $H_{t_{i+1}}$ . Assume that these Hamiltonians are related by a  $\lfloor k/2 \rfloor$ -local Hermitian operator  $\mathcal{O}_i$  in an isospectral way

$$H_{t_{i+1}} = e^{-i\mathcal{O}_i\varepsilon} H_{t_i} e^{i\mathcal{O}_i\varepsilon} \quad (2.2)$$

for some small value of  $\varepsilon$ . We are interested to see, what is the action of  $\mathcal{O}_i$  on the corresponding code spaces given by  $\mathcal{C}_{t_i}$  and  $\mathcal{C}_{t_{i+1}}$ . If both of the Hamiltonians  $H_{t_i}$  and  $H_{t_{i+1}}$  correspond to  $k$ -codes, then the rotation of the Hamiltonian acts on the space  $\mathcal{C}_{t_{i+1}}$  with the projector  $\Pi_{\mathcal{C}_{t_i}} \mathcal{O}_i$ . This gives rise to an adiabatic transport. The total evolution of the system from time 0 to time  $T$  is given by

$$U(0, T) = \mathbf{T} \lim_{N \rightarrow \infty} \prod_{i=1}^N \Pi_{\mathcal{C}} \mathcal{U}_i e^{-iH_{t=0}\Delta t} \mathcal{U}_i^\dagger \Pi_{\mathcal{C}}, \quad (2.3)$$

where  $\mathcal{U}_i = \prod_{j < i} e^{-i\mathcal{O}_j\varepsilon}$ . Assuming that the adiabaticity condition takes place at each time step, then an initially prepared system in the code space  $\mathcal{C}$  will remain there. Nevertheless, states in the code space evolve in general. One can explicitly show [19] that the operator  $U(0, T)$  evolves the code space by the Holonomy  $\Gamma_A(\gamma)$  given in (1.3) for the case of cyclic adiabatic evolutions of the Hamiltonian. Hence, by carefully engineering Hamiltonians one can obtain evolutions that give rise to an Abelian or a non-Abelian geometrical phase  $\Gamma_A(\gamma)$ . In the following we shall present a systematic way how to develop Hamiltonians that support quasiparticles with a variety of anyonic statistical behaviors.

## 2.2 Quantum Double Models

### 2.2.1 The Simple Case of the Toric Code

The toric code [13] is the simplest topological lattice model that supports Abelian anyons. It is one of the most studied topological models serving as a platform to develop new computational schemes and as a test bed to probe the properties of topological systems. It comprises of a square lattice with qubits positioned at its links and interaction terms that act at the vertices,  $A(v)$ , and plaquettes,  $B(p)$ , of the lattice. They are given by

$$A(v) = \sigma_{v,1}^x \sigma_{v,2}^x \sigma_{v,3}^x \sigma_{v,4}^x, \quad B(p) = \sigma_{p,1}^z \sigma_{p,2}^z \sigma_{p,3}^z \sigma_{p,4}^z, \quad (2.4)$$

where the indices  $1, \dots, 4$  of the Pauli operators,  $\sigma^z$  and  $\sigma^x$ , enumerate the vertices of each plaquette or vertex in a clockwise fashion. The defining Hamiltonian is

$$\mathcal{H} = - \sum_v A(v) - \sum_p B(p). \quad (2.5)$$

Each of the interaction terms commute with the Hamiltonian as well as with each other. Thus, the model is exactly solvable and its ground state is explicitly given by

$$|\text{gs}\rangle = \prod_v \frac{1}{\sqrt{2}} (\mathbb{1} + A(v)) |00\dots 0\rangle \quad (2.6)$$

with  $\sigma^z|0\rangle = |0\rangle$ . The state  $|\text{gs}\rangle$  represents the anyonic vacuum state and is unique for systems with open boundary conditions.

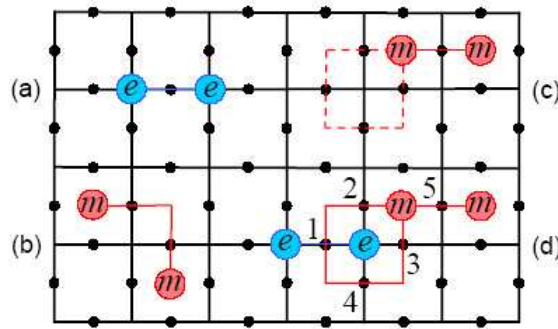


Figure 2.1: The toric code model with qubits at the links of a square lattice. Qubit rotations enable manipulations of anyons on neighboring plaquettes or vertices. (a) Application of  $\sigma^z$  on a single qubit yields two  $e$ -type anyons placed at neighboring vertices, where the string passes through the rotated qubits. Similarly,  $m$  anyons are created on plaquettes by  $\sigma^x$  rotations. (b) Two  $\sigma^x$  rotations create two pairs of  $m$ -type anyons. If one anyon from each pair is positioned on the same plaquette then they annihilate, thereby connecting their strings. (c) When a part of a string forms a loop around unpopulated plaquettes, the loop cancels (dashed). (d) Anyon  $e$  is produced by a  $\sigma^z$  on qubit 1,  $|e\rangle = \sigma_1^z |\text{gs}\rangle$ . Subsequently an  $m$  anyon is circulated around the  $e$  anyon giving rise to a non-trivial phase.

Starting from this ground state one can excite pairs of anyons connected by a string on the lattice using single qubit operations. More specifically, by applying  $\sigma^z$  on some qubit of the lattice a pair of so called  $e$ -type anyons is created on the two neighboring vertices (see Figure 2.1(a)). The system is described by the state  $|e\rangle = \sigma^z |\text{gs}\rangle$ . An  $m$  pair of anyons lives on the plaquettes and is obtained by a  $\sigma^x$  operation. The combination of both creates the composite quasiparticle  $\epsilon$  with  $|\epsilon\rangle = \sigma^z \sigma^x |\text{gs}\rangle = i \sigma^y |\text{gs}\rangle$ . These excitations are detected by measuring the eigenvalues of the corresponding  $A(v)$  or  $B(p)$  operators. Two equal Pauli rotations applied on qubits of the same plaquette or vertex create two anyons on this

plaquette or vertex, respectively. The fusion rules,  $1 \times 1 = e \times e = m \times m = \epsilon \times \epsilon = 1$ ,  $e \times m = \epsilon$ ,  $1 \times e = e$ , etc., where 1 is the vacuum state, describe the outcome from combining two anyons. In the above example, if two anyons are created on the same plaquette or vertex, then they annihilate. This operation also glues two single strings of the same type together to form a new string, again with a pair of anyons at its ends (Figure 2.1(b)). If the string forms a loop, the anyons at its end annihilate each other, thus removing the anyonic excitation. In case that only a part of the string forms a loop, the string gets truncated (Figure 2.1(c)). For non-compact systems with boundaries a string may end up at the boundary describing a single anyon at its free endpoint.

Anyonic statistics is revealed as a non-trivial phase factor acquired by the wave function of the lattice system after braiding anyons, e.g., after moving an  $m$  anyon around an  $e$  anyon (Figure 2.1(d)) or vice versa. Consider the initial state  $|\Psi_{\text{ini}}\rangle = \sigma_5^x \sigma_1^z |\text{gs}\rangle$  with neighboring  $e$  and  $m$  anyons. One  $m$  anyons is then moved around an  $e$  along the path generated by successive applications of  $\sigma^x$  rotations on the four qubits of  $v$  where  $e$  resides. The final state is

$$|\Psi_{\text{fin}}\rangle = \sigma_1^x \sigma_2^x \sigma_3^x \sigma_4^x |\Psi_{\text{ini}}\rangle = -\sigma_5^x \sigma_1^z (\sigma_1^x \sigma_2^x \sigma_3^x \sigma_4^x |\text{gs}\rangle) = -|\Psi_{\text{ini}}\rangle. \quad (2.7)$$

Such a minimal loop, which vanishes the moment it is closed, is analogous to the application of the respective interaction term  $A(v) = \sigma_{v,1}^x \sigma_{v,2}^x \sigma_{v,3}^x \sigma_{v,4}^x$  (or  $B(p) = \sigma_{p,1}^z \sigma_{p,2}^z \sigma_{p,3}^z \sigma_{p,4}^z$ ) of the Hamiltonian. This operator has eigenvalue  $+1$  for all plaquettes of the ground state  $|\text{gs}\rangle$ . It signals an excitation, e.g.  $|\Psi_{\text{ini}}\rangle$  with eigenvalue  $-1$ , when applied to the plaquette where an anyon resides, which is our case. The topological phase factor of  $-1$  reveals the non-trivial statistics between  $e$  and  $m$  anyons. However, (2.7) is much more general, as the actual path of the loop is irrelevant. It is worth noticing that the  $e$  and  $m$  anyons are distinguishable as they reside exclusively on vertices or plaquettes of the lattice, respectively. Hence, their exchange is not possible only their braiding (double exchange). This still gives a behavior that is different from the braiding of bosons or fermions. More complicated anyonic models can give rise to anyonic statistics between indistinguishable particles.

Alternatively, we can interpret (2.7) as a description of twisting  $\epsilon$ , the combination of an  $e$  and an  $m$ -type anyon, by  $2\pi$ . The phase factor of  $-1$  thereby reveals its  $4\pi$ -symmetry which is characteristic for half spin of fermionic particles [32]. Note that the  $e$  ( $m$ ) anyons exhibit bosonic statistics with respect to themselves [13].

The properties mentioned above do not need a torus configuration for the lattice Hamiltonian. This becomes necessary only when one wants to employ the toric code to encode quantum information. Indeed, non-trivial genus can give rise to degeneracy that can serve as a quantum memory. This is a general property that holds for other Abelian models as well. For example, moving from one ground state to another on a torus with genus one involves creating a pair of anyons and then moving them along non-contractible loops before re-annihilating them, as seen in Figure 2.2. Denoting two non-equivalent trajectories on the torus as 1 and 2 then one can define the states

$$|\Psi_1\rangle, |\Psi_2\rangle = C_e^1 |\Psi_1\rangle, |\Psi_3\rangle = C_e^2 |\Psi_1\rangle, |\Psi_4\rangle = C_e^1 C_e^2 |\Psi_1\rangle. \quad (2.8)$$

The operators  $C_e^1$  and  $C_e^2$  correspond to generating a pair of  $e$  anyons, moving then along the directions 1 or 2 respectively and then annihilating them. Continuously deformed

anyonic loops correspond to the same states. So only four states can be created in this way. A linearly dependent set of states can be obtained by employing the loop operators that correspond to  $m$  or combinations of  $e$  and  $m$  anyons. Hence, a four dimensional Hilbert space arises that can encode two qubits. If the toric code is defined on a surface with genus  $g$ , then it can encode  $2g$  qubits.

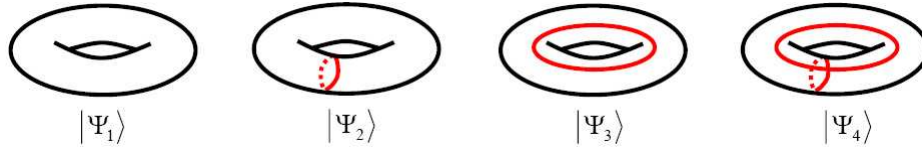


Figure 2.2: The torus with genus  $g = 1$  with the toric code model defined on it. The ground state has fourfold degeneracy  $|\Psi_i\rangle$ , for  $i = 1, \dots, 4$ . Starting from the vacuum state  $|\Psi_1\rangle$  one can create a pair of  $m$  anyons and wrap them around two non-trivial inequivalent loops on the torus giving the states  $|\Psi_2\rangle$  and  $|\Psi_3\rangle$ . State  $|\Psi_4\rangle$  corresponds to generating two inequivalent loops.

One should note the similarity with error correcting codes: the operators  $A(v)$  and  $B(p)$  are the commuting operators that detect errors, while operators that create a pair of anyons, move one of them around a non-contractible loop and re-annihilate them correspond to encoded logical gates. When anyonic errors are detected, then a string of operations is performed along the shortest distance between the anyons that annihilates them. This elimination of errors can affect the logical space only if the two errors have propagated at distance larger than  $L/2$ , where  $L$  is the linear size of the torus. In that case the error correction step might result in a non-contractible loop that corresponds to a logical gate. Hence, the toric codes corresponds to a  $[[L^2, 2, L]]$  error correcting code. With the Hamiltonian present, the generation of errors is penalized by an energy gap. Errors in the form of virtual anyonic excitations are exponentially suppressed from going around the torus. Hence, large tori sizes are favorable. Such Abelian models can serve only as memories as the encoded logical gates are not sufficient to perform universal quantum computation.

### 2.2.2 General $D(G)$ Quantum Double Models

Quantum double models are particular two dimensional lattice models with Hamiltonians that support a rich variety of anyonic excitations [13, 33]. The toric code is a special case of a quantum double model,  $D(Z_2)$ , based on the group  $Z_2 = \{1, e; e^2 = 1\}$ . In general one can take a finite group  $G$ . Consider the orthonormal basis  $\{|g\rangle : g \in G\}$  that produces a Hilbert space,  $\mathcal{H}$ , with dimensionality  $|G|$ . Assign a space  $\mathcal{H}$  to each link of the lattice which can be thought of as a spin or qudit. In the case of the toric code, this space is two dimensional corresponding to a qubit.

To define the Hamiltonian we need the linear operators  $L_+^g$ ,  $L_-^g$ ,  $T_+^h$  and  $T_-^h$  acting on  $\mathcal{H}$  with  $g, h \in G$  acting as

$$L_+^g |z\rangle = |gz\rangle, \quad L_-^g |z\rangle = |zg^{-1}\rangle, \quad T_+^h |z\rangle = \delta_{h,z} |z\rangle, \quad T_-^h |z\rangle = \delta_{h^{-1},z} |z\rangle. \quad (2.9)$$

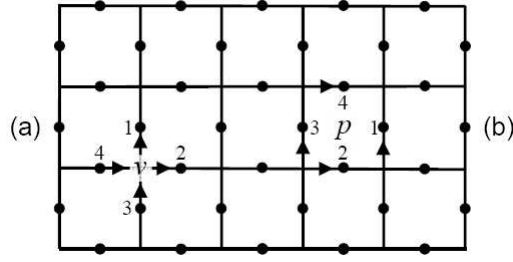


Figure 2.3: Quantum double models can be defined on a square lattice where qudits are places at the links. The lattice is oriented with vertical links pointing upwards and horizontal ones rightwards. The enumeration for the links of a vertex (a) and of a plaquette (b) is also given.

These operators satisfy the following commutation relations

$$L_+^g T_+^h = T_+^{gh} L_+^g, \quad L_-^g T_+^h = T_+^{hg^{-1}} L_-^g, \quad L_+^g T_-^h = T_-^{hg^{-1}} L_+^g, \quad L_-^g T_-^h = T_-^{gh} L_-^g. \quad (2.10)$$

Let us consider an orientation for each edge of the lattice. For concreteness we take a square lattice where the vertical links are oriented upwards and the horizontal ones rightwards, as seen in Figure 2.3. For each vertex  $v$  of the lattice we assign a vertex operator defined by

$$A(v) = \frac{1}{|G|} \sum_{g \in G} L_+^g(e_1) L_+^g(e_2) L_-^g(e_3) L_-^g(e_4), \quad (2.11)$$

where the  $e_i$ 's correspond to the four edges connected to vertex  $v$ , as seen in Figure 2.3. Similarly for a plaquette  $p$  one can define

$$B(p) = \sum_{h_1 \dots h_4=1} T_-^{h_1}(e_1) T_-^{h_2}(e_2) T_+^{h_3}(e_3) T_+^{h_4}(e_4). \quad (2.12)$$

$A(v)$  projects out states that are not gauge invariant at vertex  $v$  and  $B(p)$  projects out states with non-vanishing magnetic charge at plaquette  $p$ . All of the operators  $A(v)$ 's and  $B(p)$ 's commute with each other. Hence, the Hamiltonian

$$H = - \sum_v A(v) - \sum_p B(p) \quad (2.13)$$

is in the stabilizer formalism and can be diagonalized easily. The ground state  $|\text{gs}\rangle$  satisfies

$$A(v) |\text{gs}\rangle = |\text{gs}\rangle, \quad B(p) |\text{gs}\rangle = |\text{gs}\rangle \quad (2.14)$$

for all  $v$  and  $p$ . The excitation states of this Hamiltonian are quasi-particles that live on the vertices or the plaquettes of the lattice or simultaneously on a vertex and a neighboring plaquette, where the conditions (2.14) are violated. It is possible to find the projectors

that identify the type of quasi-particles and their properties, but this problem is complex in its generality so we shall restrict ourselves to the construction for special examples. The quasiparticles can be Abelian, arising for example from the toric code model with  $Z_2$  group, or non-Abelian arising e.g. from the  $S_3$  group.

The main property of the non-Abelian anyonic Hamiltonians that is of interest for quantum computation is their large fusion space degeneracy created by the presence of non-Abelian anyons. Their quantum information can be encoded which is protected from errors by the finite energy gap above it. Moreover, the encoding can be performed in a non-local way making it inaccessible to environmental decoherence. The advantage over the Abelian anyon encoding, as we have seen for example with the toric code, is that now one can manipulate the information by braiding the anyons together, rather than by creating anyons and circulating them around the torus. In addition, the dimension of the encoding space can be increased by creating more anyons rather than changing the topology (genus) of the surface. This dramatically simplifies the control procedure and can give rise, for certain types of non-Abelian models, to universal quantum computation.

### 2.3 Example: The $D(S_3)$ Model

Let us define the  $D(S_3)$  anyon model on an oriented two-dimensional square lattice. On each edge there resides a six-level spin spanned by the states  $|g\rangle$ , where  $g$  is an element of  $S_3$ , the permutation group of three objects. We express every element in terms of generators  $t$  and  $c$  which satisfy  $t^2 = c^3 = e$  and  $tc = c^2t$ , where  $e$  denotes the identity element. Using this notation the six elements are given by  $S_3 = \{e, c, c^2, t, tc, tc^2\}$ .

Define a vertex operator acting on vertex  $v$  by,

$$A_g(v) = L_+^g(e_1)L_+^g(e_2)L_-^g(e_3)L_-^g(e_4), \quad [A_g(v), A_h(v')] = 0, \quad (2.15)$$

where the  $e_i$  are the four edges connected to vertex  $v$  (see Fig. 2.3) and the operators  $L_\pm$  are as defined in (2.9). Similar definitions hold for the plaquette operators defined in terms of projectors onto some group element. We restrict to the set of two non-trivial anyons, which we call  $\Lambda$  and  $\Phi$ , and the vacuum,  $1$ . When  $|\Psi\rangle$  denotes a general state of the system, the presence of an anyon of type  $X$  at vertex  $v$  is defined by  $P_X|\Psi\rangle = |\Psi\rangle$ , where the orthogonal projectors are given by

$$\begin{aligned} P_1(v) &= \frac{1}{6}[A_e(v) + A_c(v) + A_{c^2}(v) + A_t(v) + A_{tc}(v) + A_{tc^2}(v)], \\ P_\Lambda(v) &= \frac{1}{6}[A_e(v) + A_c(v) + A_{c^2}(v) - A_t(v) - A_{tc}(v) - A_{tc^2}(v)], \\ P_\Phi(v) &= \frac{1}{3}[2A_e(v) - A_c(v) - A_{c^2}(v)]. \end{aligned}$$

Projectors can also be defined for anyons on plaquettes, but we shall not give them here.

Define now the projector to the vacuum states of the vertices with  $A(v) = P_1(v)$  and similarly with  $B(p)$  for the plaquettes. The stabilizer space consists of states with no anyons, i.e. those for which  $A(v)|gs\rangle = |gs\rangle$  for all  $v$ , and  $B(p)|gs\rangle = |gs\rangle$  for all  $p$ . The

syndrome measurement is defined as a measurement of anyon occupancies and corresponds to the above projectors. A Hamiltonian may be defined to protect the stabilizer space. This assigns energy to the states of the anyons, and thus suppresses their spontaneous creation. Thus, the Hamiltonian is expressed by

$$H = - \sum_v A(v) - \sum_p B(p). \quad (2.16)$$

Anyons on the vertices are created from the stabilizer space by acting with the following operators on single spins,

$$W_\Lambda(e) = |e\rangle \langle e| + |c\rangle \langle c| + |c^2\rangle \langle c^2| - |t\rangle \langle t| - |tc\rangle \langle tc| - |tc^2\rangle \langle tc^2|, \quad (2.17)$$

$$W_\Phi(e) = 2|e\rangle \langle e| - |c\rangle \langle c| - |c^2\rangle \langle c^2|. \quad (2.18)$$

These create anyons on the two vertices connected by the edge  $e$ . A protocol to move anyons several edges apart is given in [35, 36]. When anyons of different type are brought to the same vertex, the possible outcomes are given by the fusion rules

$$\Lambda \times \Lambda = 1, \quad \Lambda \times \Phi = \Phi, \quad \Phi \times \Phi = 1 + \Lambda + \Phi. \quad (2.19)$$

The last implies that the  $\Phi$  anyons have three possible fusion channels: a pair may fuse to the trivial anyon 1, a  $\Lambda$  or a  $\Phi$ . One can verify these fusion rules from the creation operators (2.18) of the anyons. Consider a certain link  $e$ . Then  $W_\Lambda(e)W_\Phi(e) = W_\Phi(e)$  which demonstrates that creating a  $\Lambda$  and a  $\Phi$  anyon on the same vertex (here on two neighboring vertices) is equivalent as having only a  $\Phi$  anyon on that vertex. Moreover,  $W_\Phi(e)W_\Phi(e) = 4|e\rangle \langle e| + |c\rangle \langle c| + |c^2\rangle \langle c^2|$ . On the other hand one can show that  $W_1(e) + W_\Lambda(e) + W_\Phi(e) = 4|e\rangle \langle e| + |c\rangle \langle c| + |c^2\rangle \langle c^2|$ . Hence  $W_\Phi(e)W_\Phi(e) = W_1(e) + W_\Lambda(e) + W_\Phi(e)$  demonstrating the possible presence of all particles, 1,  $\Lambda$  and  $\Phi$  on either vertices.

We can utilize the encoding of topological quantum computation, associating each possible outcome with a quantum state and hence using them to store quantum information. This information will be topologically protected due to a finite energy gap and non-local encoding. However, the anyons have trivial mutual statistics meaning that information processing by purely topological means is not possible. To achieve universal quantum computation one can additionally employ non-topological operations, such as spin measurements, to harness the power of the underlying spin lattice [37].

## 2.4 Exercises

- **Exercise 1:** Develop explicitly the Quantum Double theory for the  $Z_2$  group.  $D(Z_2)$  is the toric code.
- **Exercise 2:** Demonstrate the anyonic properties of the Abelian  $D(Z_n)$  model.
- **Exercise 3:** Write down all the anyonic particles for  $D(S_3)$  and demonstrate their non-Abelian fusion and statistics.



## Chapter 3

# Jones Polynomials

### 3.1 A New Quantum Algorithm!

The study of anyonic systems for performing quantum computation has led to the exciting discovery of a new quantum algorithm that evaluates the Jones polynomials [38]. These polynomials are topological invariants of knots and links. They were first connected to topological quantum field theories by Witten [26]. Since then they have found far reaching applications in various areas such as in biology for DNA reconstruction and in statistical physics [39]. The best known classical algorithm for the exact evaluation of Jones polynomials demands exponential resources [40]. Employing anyons only a polynomial number of resources is required to produce an approximate answer of this problem [41]. The techniques used by manipulating anyons resemble an analogue computer. Indeed, the idea is equivalent to the classical setup, where a wire is wrapped several times around a solenoid that confines magnetic flux: by measuring the current that runs through the wire one can obtain the number of times the wire was wrapped around the solenoid. The translation of the corresponding anyonic evolution to a quantum algorithm was explicitly demonstrated in [42].

### 3.2 Braid Group and Traces

To better understand the structure of the computation, let us first introduce a few necessary elements. The main mathematical structure behind the evolution of anyons is the braid group  $B_n$  on  $n$  strands. Its elements  $b_i$  for  $i = 1, \dots, n - 1$  can be viewed as braiding the world lines of anyons. Specifically, if  $n$  anyons are placed in a certain order, then the element  $b_i$  describes the effect of exchanging the position of anyons  $i$  and  $i + 1$ , e.g. in a counterclockwise fashion. Thus all possible manipulations between the anyons can be written as a combination of the  $b_i$ 's. The elements of the group  $B_n$  satisfy the following relations

$$\begin{aligned} b_i b_j &= b_j b_i, & \text{for } |i - j| \geq 2 \\ b_i b_{i+1} b_i &= b_{i+1} b_i b_{i+1}, & \text{for } 1 \leq i < n \end{aligned} \tag{3.1}$$

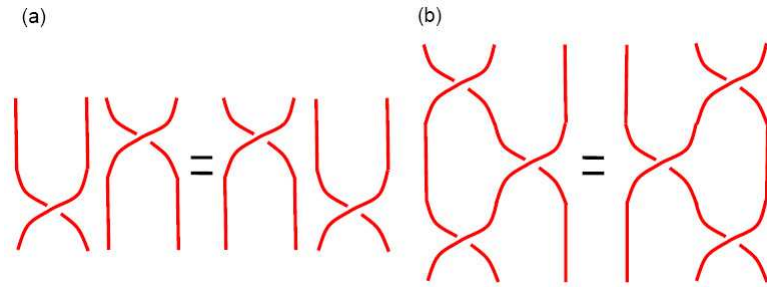


Figure 3.1: Connection between braids and knots. (a) Schematic representation of the relation  $b_i b_j = b_j b_i$  when  $|i - j| \geq 2$ . Exchanging the order of two braids does not have an effect if they are sufficiently far apart. (b) Schematic representation of the relation  $b_i b_{i+1} b_i = b_{i+1} b_i b_{i+1}$  for  $1 \leq i < n$ . The two braidings are equivalent under simple continuous deformations.

. These relations have a simple geometrical meaning, presented in Figure 3.1. Note that the symmetric group  $S_n$  is a representation of  $B_n$ , if we impose the condition  $b_j^2 = 1$  for all  $j$ . This would be true for boson and fermions, where  $b_j = \pm 1$ . As discussed earlier, in two dimensions other possibilities arise.

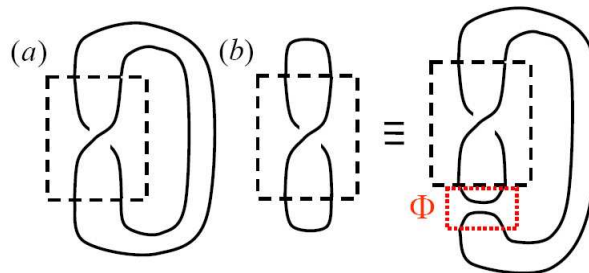


Figure 3.2: (a) The Markov trace performed by linking the opposite ends of the strands. (b) The Plat trace connects pairwise neighboring strands. The Plat trace can be expressed as a Markov trace with the addition of the  $\Phi$  graph element.

The next element we need for the quantum algorithm is the introduction of a trace that establishes the equivalence between braidings and knots or links. A version of this tracing procedure called the Markov trace consists of connecting the opposite endpoints of the braids together, as shown in Figure 3.2(a). Alternatively, one might connect neighboring strands in a pairwise fashion. This gives rise to the Plat trace shown in Figure 3.2(b). Hence, a braid with a trace gives a knot or a link. Surprisingly, every knot or link is equivalent to a braid with a trace due to Alexander's theorem [43]. Hence, one can simulate a knot or a link by simply braiding anyons of the same type.

### 3.3 Reidemeister Moves and Skein Relations

To demonstrate the relation between anyons and the Jones polynomials we need to introduce a way of assigning topological invariant polynomials to links. First we need to define equivalency classes between links that can be continuously deformed into each other. Surprisingly three elementary moves are sufficient to establish these equivalencies. They are called the Reidemeister moves depicted in Figure 3.3. Topologically equivalent links can be related by these moves.

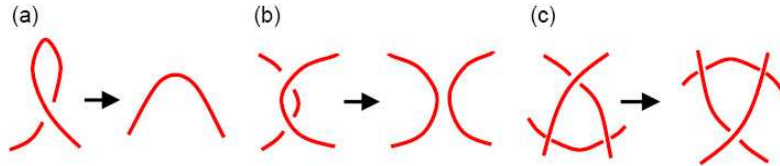


Figure 3.3: (a) The first Reidemeister move undoes a twist. (b) The second Reidemeister move separates two unbraided strands. (c) The third Reidemeister move slides a strand under a crossing.

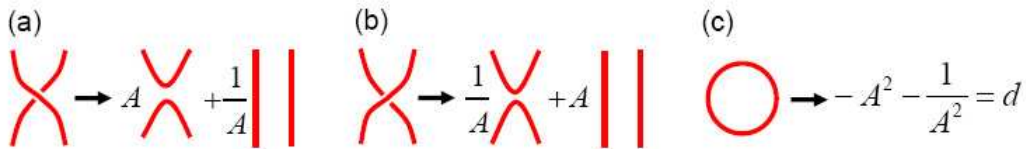


Figure 3.4: (a) and (b) depict the Skein relations. (c) For every closed loop we assign the number  $d$ .

Next we want to assign polynomials to links that are insensitive to Reidemeister moves. As seen in Figure 3.4(a,b), the Skein relations reduce the crossings of the links to a combination of avoided crossings and coefficients parameterized by  $A$ . If this is applied to all crossings, then the only left components are unlinked loops. By substituting each loop with  $d$  as seen in Figure 3.4(c) we obtain a Laurent polynomial in  $A$ . This polynomial is called the Kauffman bracket  $\langle L \rangle(A)$  of the link  $L$ . Kauffman brackets have the following properties  $\langle LO \rangle = d \langle L \rangle$  for  $L$  being a general non-empty link and  $O$  being the trivial link, while  $\langle O \rangle = 1$ .

One can show that the Kauffman bracket satisfies the Reidemeister moves (a,b). Indeed, by employing the Skein relations we see that the last two Reidemeister moves are identically satisfied. To satisfy the first Reidemeister move one needs to rescale the Kauffman bracket

in the following way

$$V_L(A) = (-A)^{3w(L)} \langle L \rangle(A) \quad (3.2)$$

The parameter  $w(L)$  is the writhe or twist of the link. For an oriented link assign a  $+1$  to a clockwise crossing and a  $-1$  to an anticlockwise crossing. The writhe is then the sum of these signs for all crossings. One can show that the Jones polynomial,  $V_L(A)$ , is an invariant with respect to the first Reidemeister move. It is hence a topological invariant of links.

Finally, one can show that the trace of unitary representations of the braiding group corresponds to the Kauffman bracket of the Markov trace of braided strands [42]. Thus one has

$$\text{tr}(B(A)) = \langle (B)^{\text{Markov}} \rangle(A), \quad (3.3)$$

where the braid  $B$  has been Markov traced and then the corresponding Kauffman bracket has been evaluated.

### 3.4 Analog Evaluation of Jones Polynomials

Consider the following anyonic evolution. Create  $n$  anyons of quantum dimension  $d$  from the vacuum state in pairs. In the following,  $|\alpha\rangle$ , denotes the fusion state corresponding to the case where the fusion of the anyons in the pairwise fashion in which they were created results in the vacuum for each pair. Assume we perform an arbitrary braiding  $B$  among these anyons before we pairwise fuse them with the same ordering as the pair creation. The probability of obtaining the vacuum state at the final fusion is a measurable quantity given by

$$\langle \alpha | B(A) | \alpha \rangle = \frac{1}{d^{n/2-1}} \langle (B)^{\text{Plat}} \rangle(A). \quad (3.4)$$

Here  $B$  has been Plat traced and then the corresponding Kauffman bracket has been evaluated. Hence one can obtain the Kauffman bracket from the probability of finally obtaining the vacuum state. The evaluation of the writhe is a polynomially easy task. So the above prescription efficiently gives the Jones polynomial. The choice of braid representation  $B(A)$ , associated to a particular type of anyons, depends on the parameter  $A$  that also appears as a variable of the Jones polynomial.

The Jones polynomial has been shown to be a topological invariant [38], i.e. its value for a given link  $L$  is unchanged under continuous deformations. Consider two links  $L_1$  and  $L_2$ . If  $V_{L_1} \neq V_{L_2}$  then  $L_1$  and  $L_2$  are inequivalent, i.e. they cannot be mapped to each other by continuous deformations. Note, however, that inequivalent links may have the same Jones polynomial. Computation of the Jones polynomial by a classical computer appears to be exponentially hard due to the fact that there are exponentially many terms to sum and no closed form for the number of loops as a function of the resolution of the link exists. On the other hand it is rather easy to approximate its value by employing anyons. The translation of the anyonic evolution to algorithms was performed by Aharonov, Jones and Landau in [42].

### 3.5 Example: A Simple Link

For illustration we sketch the quantum algorithm that evaluates the Jones polynomial for the three strand braid group  $B_3$  (see also [44]). First one picks a representation of the braid group. A simple non-Abelian representation is given by  $2 \times 2$  matrices which can be parameterized as:  $\Gamma(b_j) = A\mathbf{1}_2 + \frac{1}{A}V_j$  where

$$V_1 = \begin{pmatrix} d & 0 \\ 0 & 0 \end{pmatrix}, \quad V_2 = \begin{pmatrix} d^{-1} & \sqrt{1-d^{-2}} \\ \sqrt{1-d^{-2}} & d-d^{-1} \end{pmatrix}. \quad (3.5)$$

In this case  $\Gamma(b_1)\Gamma(b_2)\Gamma(b_1) = \Gamma(b_2)\Gamma(b_1)\Gamma(b_2)$ . The set  $\{\mathbf{1}_2, V_1, V_2, V_1V_2, V_2V_1\}$  obeys the braiding identities of (3.1) and satisfies  $V_1V_2V_1 = V_1$ ,  $V_2V_1V_2 = V_2$ . The representation becomes unitary if we choose  $A = e^{i\theta/4}$  for  $|\theta| \leq 2\pi/3$  or  $|\theta/4 + \pi| \leq \pi/6$ . Any sequence of  $k$  braids can be described by a braid word  $r = r_1r_2 \dots r_k$ . This word has a closure which corresponds to a link  $L_r$ . For  $B_3$  we have  $r_k \in \{b_1, b_2\}$  so  $\langle L_r \rangle = \langle \prod_{j=1}^k \Gamma(r_j) \rangle = \langle A^k \mathbf{1}_2 \rangle + \langle F(r) \rangle$ , where  $F(r)$  is a sum of products of the matrices  $V_1, V_2$ . The closure of the identity operation on  $B_3$  represents three closed loops hence  $\langle \mathbf{1}_2 \rangle = d^2$ . The bracket of the closure of a braid word is a function computed by taking the trace over the carrier space of the representation and we have  $\langle L_r \rangle(t) = A^k(d^2 - 2) + \text{Tr}[\prod_{j=1}^k \Gamma(r_j)]$ . By direct measurement of the anyons it is possible to determine the value of the Jones polynomial.

By the above analysis the difficulty of computing the Jones polynomial is reduced to computing the trace of a product of unitaries. Good quantum algorithms exist for computing traces of unitaries. For example, one can begin with a completely mixed state of  $n$  register qubits and one work qubit  $w$  prepared in the pure state  $(|0\rangle_w + |1\rangle_w)/\sqrt{2}$ . Applying a sequence of controlled unitaries  $\prod_{j=1}^k |1\rangle_w \langle 1| \otimes \Gamma(r_j)$  and measuring the work qubit in the  $\hat{x}$  and  $\hat{y}$  bases outputs, one obtains the real and imaginary parts of the normalized trace  $\text{Tr}[\prod_{j=1}^k \Gamma(r_j)]/2^n$ .

### 3.6 Exercises

- **Exercise 1:** Demonstrate that the last two Reidemeister moves are compatible with the Skein relations.
- **Exercise 2:** Demonstrate that the Jones polynomials are invariant under the first Reidemeister move. For that you might need to first check how the Skein relations reduce a single twist.
- **Exercise 3:** Demonstrate that the trace of a braiding corresponds uniquely to the Markov trace.
- **Exercise 4:** Demonstrate how one can obtain relation (3.4) from (3.3).
- **Exercise 5:** Demonstrate that the Kauffman bracket of the trefoil is given by  $A^5 + A^3 - A^{-7}$ .



# Chapter 4

## Outlook

### 4.1 Topological Entropy

In order to perform topological quantum computation one first needs to identify if a certain medium has topological properties. As topological properties are non-local in nature we cannot expect a local order parameter to be adequate. Hamma, Ionicioiu and Zanardi [45] revealed entropic properties of the toric code ground states that are unique, due to their topological character. Subsequently, Kitaev and Preskill [46] and simultaneously Levin and Wen [47] introduced the concept of topological entropy that distinguishes if a system is topologically ordered or not. We shall briefly review these constructions.

Consider a pure system prepared in its ground state and a bipartition in  $R$  and its complement  $\bar{R}$  that are separated by the boundary  $\partial R$ . Denote by  $\rho_R$  the reduced density matrix of  $R$ . Assume that its von Neumann entropy  $S_R = -\text{tr}(\rho_R \ln \rho_R)$  satisfies

$$S_R = \alpha |\partial R| - \gamma + \epsilon(|\partial R|), \quad (4.1)$$

where  $\epsilon(|\partial R|)$  tends to zero as the size of the boundary,  $|\partial R|$ , tends to infinity. The von Neumann entropy does not have a ‘volume’ term as it corresponds to a pure state, while the area law is generically expected for a gapped system. As discussed in [45, 46, 47], systems with non-zero  $\gamma$  are topologically ordered. Indeed,  $\gamma$  is related to the total topological dimension  $\mathcal{D}$  of the model, i.e.

$$\gamma = \ln \mathcal{D} = \ln \sqrt{\sum_q d_q^2}, \quad (4.2)$$

where  $d_q$  is the quantum dimension associated with anyon  $q$ . When the system does not possess anyons, then  $\mathcal{D} = 1$  as it gets contributions only from the vacuum, giving  $\gamma = 0$ .

One can isolate the constant term from the von Neumann entropy in two different ways. Consider a system defined on a closed surface  $\Sigma$ , e.g. a sphere, admitting the partition in four areas,  $A$ ,  $B$ ,  $C$  and  $D$ , as seen in Figure 4.1. Then  $\gamma$  can be obtained from the following linear combination of entropies [46]

$$\gamma = S_A + S_B + S_C - S_{AB} - S_{AC} - S_{BC} + S_{ABC}. \quad (4.3)$$

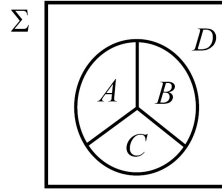


Figure 4.1: The surface  $\Sigma$  partitioned in the areas  $A$ ,  $B$ ,  $C$  and  $D$ .

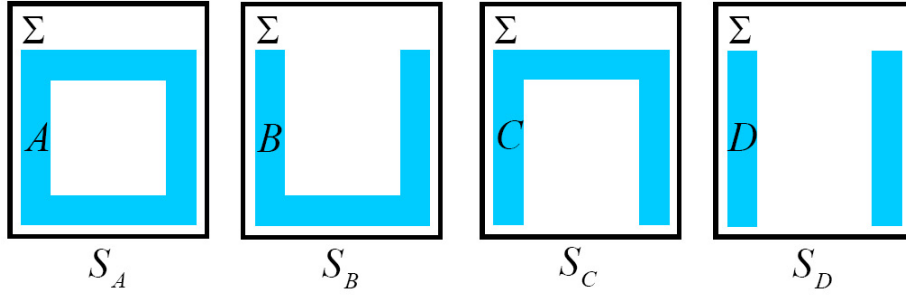


Figure 4.2: The surface  $\Sigma$  partitioned in four different ways,  $A$ ,  $B$ ,  $C$  and  $D$  with corresponding von Neumann entropies  $S_A$ ,  $S_B$ ,  $S_C$  and  $S_D$  respectively.

This can be demonstrated from a direct substitution of (4.1). The entropy  $S_{AB}$  is evaluated for the composite area of  $A$  and  $B$ . Alternatively, one can evaluate the entropy for the areas depicted in Figure 4.2. The constant part can be isolated by the following combination

$$\gamma = -\frac{1}{2} \left[ (S_A - S_B) - (S_C - S_D) \right]. \quad (4.4)$$

Note that these are different partitions of the same system rather than parts of the same partition as employed in (4.3). Both relations are exact in the limit where all the involved areas  $R$  are large enough so that  $\epsilon(|\partial R|) \rightarrow 0$ .

The latter method gives an intuitive picture for the topological character of  $\gamma$ . As the system is gapped the von Neumann entropies obtain in general contributions from short range correlations. The difference  $S_A - S_B$  has contributions that come from the upper horizontal part of the area  $A$ . Similarly, the contributions from  $S_C - S_D$  come from the a similar upper part. Hence, their difference should go to zero when the respective areas become sufficiently large. The only possible contribution could arise from a non-local operator, like a loop that wraps non-trivially around the area  $A$ . This contribution can not be cancelled from the entropies of  $S_B$ ,  $S_C$  or  $S_D$ ; hence it results in a non-zero value of  $\gamma$ . Such a contribution is indeed possible if the system is topologically ordered.

## 4.2 Topological Memories

As topological systems can store information in an efficient way, they have been considered as quantum memories. Indeed, it has been discussed how virtual local excitations are suppressed due to the finite energy gap that protects non-locally encoded information. If errors happen in a probabilistic way, e.g. in the presence of a non-zero temperature, then topological models seem to be weak in fighting decoherence. By studying the behavior of the topological entropy  $\gamma$  against probabilistic errors it has been shown that finite temperature destroys the topological order of a system in general [48, 49, 50]. In other words, a finite probability of anyon generation in a system will generally alter the encoded quantum information.

Lately, several models have been presented to combat temperature errors. Their goal is to slightly alter topological models in order to recover a decoherence time that increases with the size of the system (the system is hence stable in the thermodynamic limit), or at least remains finite, but large. General limits on the passive protection of quantum information by Hamiltonians is given in [51]. Recently, Hamma, Castelnovo and Chamon [52] demonstrated that if one couples the toric code appropriately with phonon fields then attractive interactions between anyons are created that increase logarithmically with their distance. This will eventually suppress the generation of unwanted anyons and their propagation around the system that destroys the encoded information. An alternative method was presented by Chesi, Roethlisberger and Loss [53]. They demonstrated that polynomially repulsive interactions between the toric code anyons suppress thermal errors efficiently. Both of these models need either detailed engineering or long range interactions to become effective so they are rather hard to implement physically. It is a fascinating current topic of research to establish whether or not it is possible to engineer a quantum memory that can protect against errors in an efficient way.

In parallel a number of algorithms have been developed that aim to combat thermal errors that are inspired from topological models. For example, one could employ error correction in order to combat the loss of physical qubits from the topological system [54]. Alternative methods, that do not rely on a Hamiltonian are given by Raussendorf and Harrington [55]. They proposed a one-way quantum computation scheme integrated with topological quantum computation and magic state distillation [56] that manages to achieve an error threshold of 0.75%. This is a very successful scheme that significantly narrows the gap between theoretical constraints and experimental abilities for the performance of quantum computation.

## 4.3 Anyons: Where Are They?

One can easily recognize the significance of topological systems for performing fault-tolerant quantum computation. There are two main categories of physical proposals for the realization of two dimensional topological systems. Systems that are defined on the continuum and discrete systems. It is natural to ask, which are the most promising architectures for realizing them in the laboratory. Undoubtable the Fractional Quantum Hall Effect is so

far the most developed area. It is concerned with a two dimensional cloud of electrons in the presence of a strong perpendicular magnetic field. There is a big variety of topological phases that arise as a function of the magnetic field and the density of electrons [57]. The most striking characteristic is that the system behaves as if it is composed of fractions of the electron charge. This was first demonstrated experimentally by Tsui, Stormer and Gosard [58] and it was theoretically explained by Laughlin [4]. Alternative systems are the  $p_x + ip_y$  superconductors that can support fractional vortices with anyonic statistics [59, 60]. Recently, topological insulators came into play where they present similar properties as the fractional quantum Hall effect without the presence of a magnetic field [61].

Alternative to the continuum cloud of electrons one can consider two dimensional lattice systems. The quantum double models presented in Chapter 2 have been proposed to be realized with Josephson junctions [62]. First experimental results for the toric code have already appeared [63] where the four spin interaction terms are realized. The demonstration of the anyonic statistics in the toric code has performed with four photons [64] and six photons [65]. A drawback of these models is the need for many body interactions. A non-Abelian anyonic model that requires only two body interactions has been presented by Kitaev [24]. A Proposal for its realization with cold atoms was given by Duan, Demler and Lukin [66] and with polar molecules by Micheli, Brennen and Zoller [67].

## 4.4 Exercises

- **Exercise 1:** Demonstrate relation (4.2).
- **Exercise 2:** Demonstrate relation (4.3).
- **Exercise 3:** Demonstrate relation (4.4).

# Bibliography

- [1] J. M. Leinaas and J. Myrheim, *Nuovo Cimento B* **37**, 1 (1977).
- [2] F. Wilczek, *Phys. Rev. Lett.* **49**, 957 (1982).
- [3] D. C. Tsui, H. L. Stormer and A. C. Gossard, *Phys. Rev. Lett.* **48**, 1559 (1982).
- [4] R. B. Laughlin, *Phys. Rev. Lett.* **50**, 1395 (1983).
- [5] F. E. Camino, W. Zhou and V.J. Goldman *Phys. Rev. Lett.* **98**, 076805 (2007).
- [6] E. Rowell, R. Stong and Z. Wang, arXiv:0712.1377 (2007).
- [7] M. A. Nielsen and I. L. Chuang, *Quantum Computation and Quantum Information*, (Cambridge, 2000).
- [8] L. K. Grover, 28th Annual ACM Symposium on the Theory of Computing, p. 212 (1996).
- [9] P. Shor, *SIAM J. Comput.* **26**, 1484 (1997).
- [10] R. Raussendorf and H.-J. Briegel, *Phys. Rev. Lett.* **86**, 5188 (2001).
- [11] E. Farhi, J. Goldstone, S. Gutmann, J. Lapan, A. Lundgren and D. Preda, *Science* **292**, 472 (2001).
- [12] G. Castagnoli and M. Rasetti, *Int. J. of Mod. Phys.* **32**, 2335 (1993).
- [13] A. Kitaev, *Annals Phys.* 303, 2 (2003).
- [14] P. Shor, *Phys. Rev. A* **52**, 2493 (1995).
- [15] A. M. Steane, *Phys. Rev. Lett.* **77**, 793 (1996).
- [16] Y. Aharonov and D. Bohm, *Phys. Rev.* **115**, 485 (1959).
- [17] Z. Nussinov and G. Ortiz, *Proc. Nat. Ac. Sc. USA* **106**, 16944 (2009).
- [18] M. V. Berry, *Roc. R. Soc. A* **392**, 45 (1984).
- [19] J. K. Pachos and P. Zanardi, *Int. J. Mod. Phys. B* **15**, 1257 (2001).

- [20] F. Wilczek and A. Zee, Phys. Rev. Lett. **52**, 2111 (1984).
- [21] D. Arovas, J.R. Schrieffer and F. Wilczek, Phys. Rev. Lett **53**, 722 (1984).
- [22] N. Read, Phys. Rev. B **79**, 045308 (2009).
- [23] V. Lahtinen and J. K. Pachos, New J. Phys. **11**, 093027 (2009).
- [24] A. Kitaev, Annals of Physics **321**, 2 (2006).
- [25] V. G. Turaev, Quantum invariants of knots and 3-manifolds, de Gruyter Studies in Mathematics 18, Walter de Gruyter & Co. (1994).
- [26] E. Witten, Commun. Math. Phys. **121**, 351 (1989).
- [27] D. Finkelstein and J. Rubinstein, J. Math. Phys. **9**, 1762 (1968).
- [28] J. Preskill, Lecture Notes for Physics 219: Quantum Computation, <http://www.theory.caltech.edu/~preskill/> (2004).
- [29] M. Freedman, M. Larsen and Z. Wang, Comm. Math. Phys. **228**, 177 (2002).
- [30] S. Bravyi, Phys. Rev. A **73**, 042313 (2006).
- [31] D. Gottesman, Phys. Rev. A **57**(1998), 127-137.
- [32] H. Rauch, *et al.* Phys. Lett. A **54**, 425 (1975).
- [33] F. A. Bais, P. van Driel and M. de Wild Propitius, Phys. Lett. B **280**, 63 (1992).
- [34] M. H. Freedman, A. Kitaev, M. J. Larsen, and Z. Wang Bull. Amer. Math. Soc. **40**, 31 (2003).
- [35] M. Aguado, G. K. Brennen, F. Verstraete and J. I. Cirac, Phys. Rev. Lett. **101**, 260501 (2008).
- [36] G. K. Brennen, M. Aguado, and J. I. Cirac, New Jour. Phys. **11**, 053009 (2009).
- [37] J. R. Wootton, V. Lahtinen and J. K. Pachos, proceedings of Theory of Quantum Computation, Communication and Cryptography, 2009, arXiv:0906.2748 (2009).
- [38] V. F. R. Jones, Bull. Amer. Math. Soc. **12**, 103 (1985).
- [39] L.H. Kauffman, *Knots and Physics*, World Scientific, Singapore (1991).
- [40] F. Jaeger, D. L. Vertigan and D. J. A. Welsh, Math. Proc. Cambridge Phil. Soc. **108**, 35 (1990).
- [41] M. H. Freedman, A. Kitaev, M. J. Larsen and Z. Wang, Bull. Amer. Math. Soc. **40**, 31 (2003).

- [42] D. Aharonov, V. Jones and Z. Landau, *Algorithmica* **55**, 395 (2009).
- [43] J. W. Alexander, *Proc. Nat. Acad. Sci.*, **9**, 93 (1923).
- [44] L. H. Kauffman and S. Lomanaco, *quant-ph/0606114* (2006).
- [45] A. Hamma, R. Ionicioiu and P. Zanardi, *Phys. Lett. A* **337**, 22 (2005).
- [46] A. Kitaev and J. Preskill, *Phys. Rev. Lett.* **96**, 110404 (2006).
- [47] M. Levin and X.-G. Wen, *Phys. Rev. Lett.* **96**, 110405 (2006).
- [48] C. Castelnovo and C. Chamon, *Phys. Rev. B* **76**, 184442 (2007).
- [49] S. Iblisdir, D. Prez-Garca, M. Aguado and J. K. Pachos, *Phys. Rev. B* **79**, 4303 (2009); to appear in *Nuc. Phys. B*, arXiv:0812.4975 (2008).
- [50] S. B. Chung, H. Yao, T. L. Hughes and E.-A. Kim, arXiv:0909.2655 (2009).
- [51] F. Pastawski, A. Kay, N. Schuch and I. Cirac, arXiv:0911.3843 (2009).
- [52] A. Hamma, C. Castelnovo and C. Chamon, *Phys. Rev. B* **79**, 245122 (2009).
- [53] S. Chesi, B. Roethlisberger and D. Loss, arXiv:0908.4264 (2009).
- [54] T. M. Stace, S. D. Barrett, and A. C. Doherty, *Phys. Rev. Lett.* **102**, 200501 (2009).
- [55] R. Raussendorf, S. Bravyi and J. Harrington, *Phys. Rev. A* **71**, 062313 (2005).
- [56] S. Bravyi and A. Kitaev, *Phys. Rev. A* **71**, 022316 (2005).
- [57] C. Nayak, S. H. Simon, A. Stern, M. Freedman and S. Das Sarma, *Rev. Mod. Phys.* **80**, 1083 (2008).
- [58] D. C. Tsui, H. L. Stormer and A. C. Gossard, *Phys. Rev. Lett.* **48**, 1559 (1982).
- [59] N. Read and D. Green, *Phys. Rev. B* **61**, 10267 (2000).
- [60] D. A. Ivanov, *Phys. Rev. Lett.* **86**, 268 (2001).
- [61] C. L. Kane, E. J. Mele, *Science* **314**, 1692 (2006).
- [62] B. Doucot, L.B. Ioffe and J. Vidal, *Phys.Rev. B* **69**, 214501 (2004).
- [63] S. Gladchenko, D. Olaya, E. Dupont-Ferrier, B. Doucot, L. B. Ioffe and M. E. Gershenson, arXiv:0802.2295 (2008).
- [64] J. K. Pachos, W. Wieczorek, C. Schmid, N. Kiesel, R. Pohlner and H. Weinfurter, *New J. Phys.* **11**, 083010 (2009).
- [65] C.-Y. Lu, *et al.*, *Phys. Rev. Lett.* **102**, 030502 (2009).
- [66] L.-M. Duan, E. Demler and M. D. Lukin, *Phys. Rev. Lett.* **91**, 090402 (2003).
- [67] A. Micheli, G. K. Brennen and P. Zoller, *Nature Physics* **2**, 341 (2006).